Modelling particle-particle and particle-fluid interactions in DEM

Colin Thornton

School of Engineering

University of Birmingham

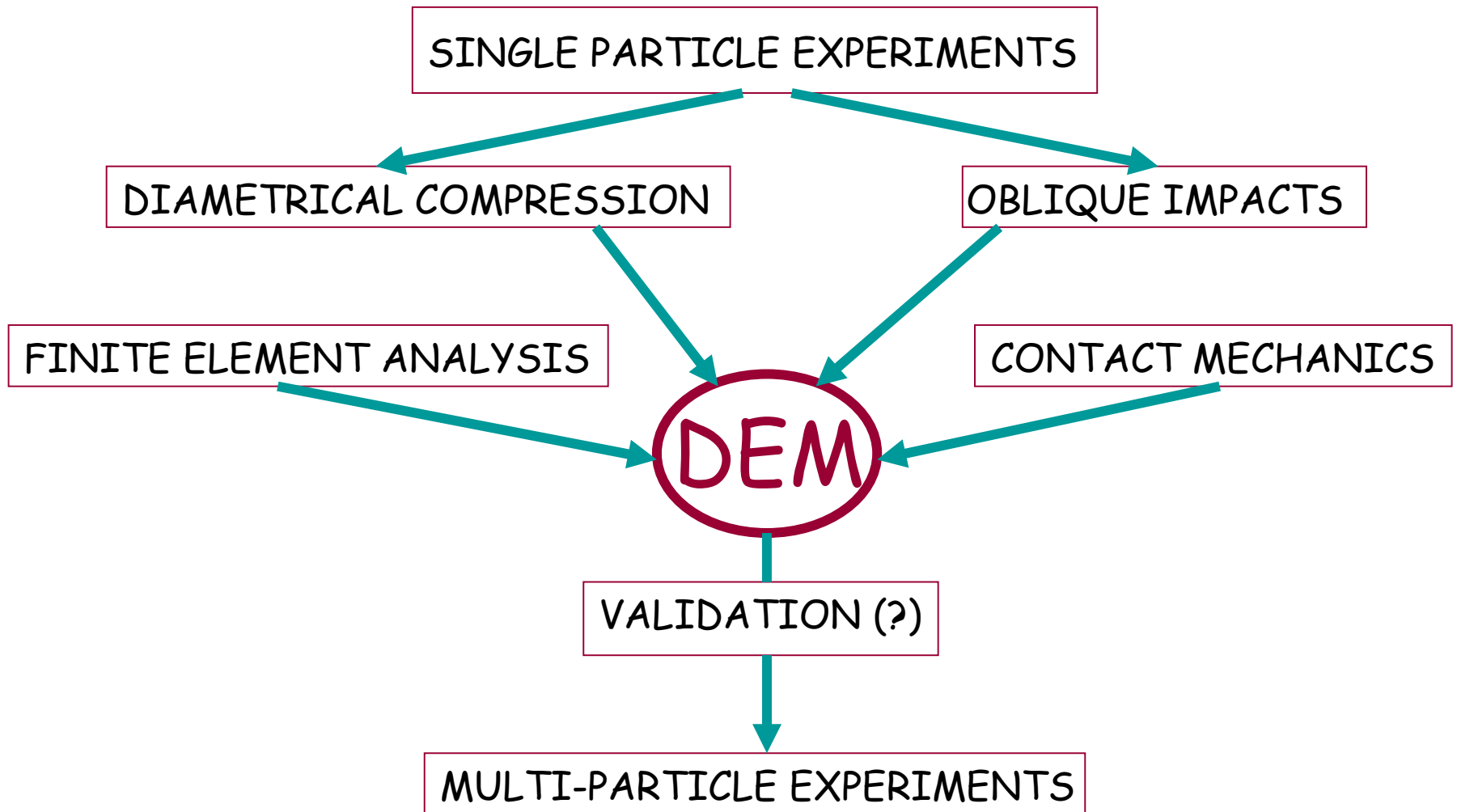PARDEM Workshop, Nuremberg, 28th March 2007

Outline

1. PARTICLE-PARTICLE INTERACTIONS

    (i)   Elastic
    (ii) Elastic-perfectly plastic
    (iii) Autoadhesive
    (iv) Liquid bridges

2. PARTICLE-FLUID INTERACTIONS

All restricted to spherical particles !

OVERVIEW

ELASTIC CONTACT INTERACTIONS

Normal interaction   (Hertz, 1896)

$$N = \frac{4}{3} E^* \left(R^* \alpha^3 \right)^{1/2}$$
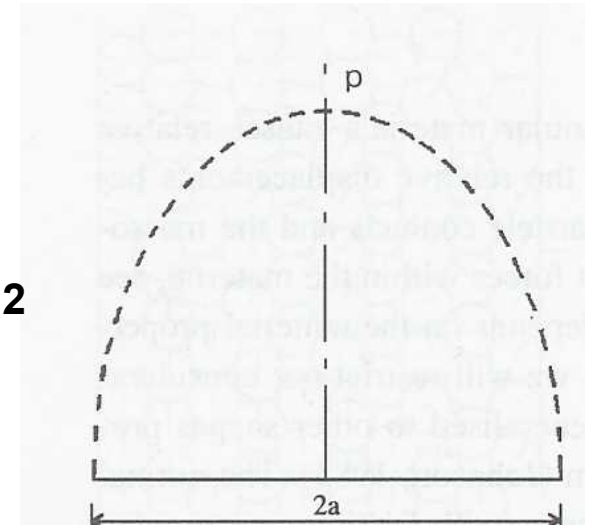
$$a = \left(\frac{3NR^*}{4E^*} \right)^{1/3}$$

$$p(r) = p_0 \left[1 - \left(\frac{r}{a} \right)^2 \right]^{1/2}$$

$$p_0 = \frac{3N}{2\pi a^2}$$

pressure distribution

$$a^2 = R^* \alpha$$

$$k_n = 2E^* a$$

$$\frac{1}{R^*} = \frac{1}{R_1} + \frac{1}{R_2}$$

$$\frac{1}{E^*} = \frac{\left(1 - \nu_1^2 \right)}{E_1} + \frac{\left(1 - \nu_2^2 \right)}{E_2}$$
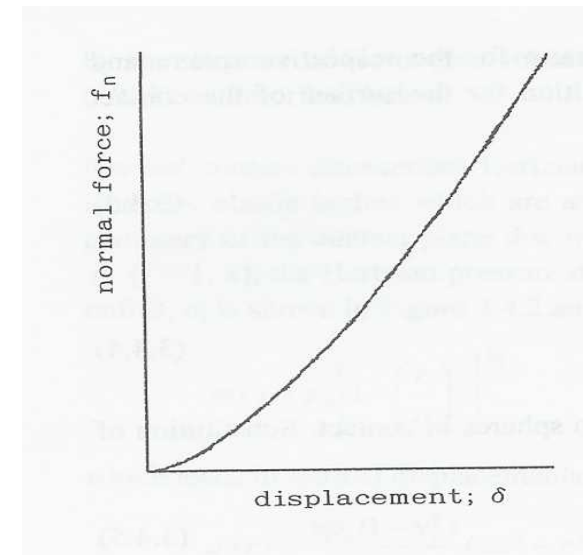
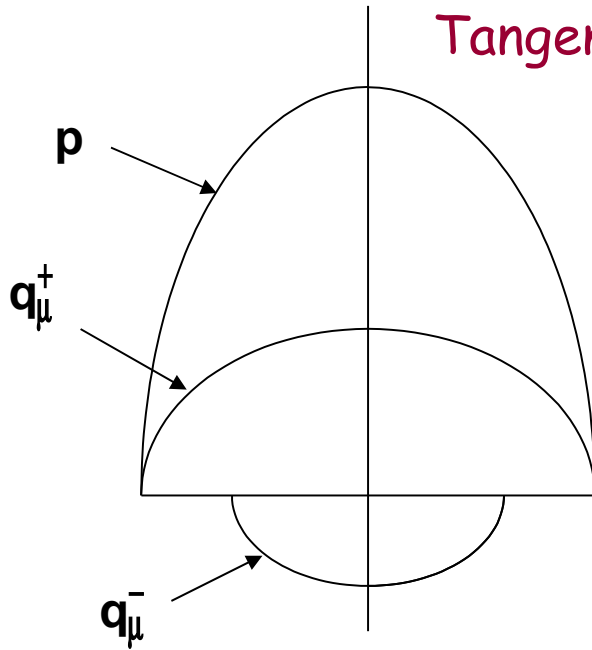**force-displacement**

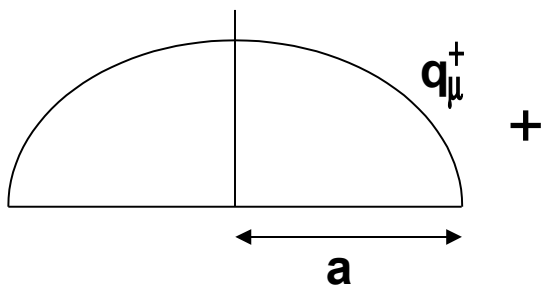# Tangential interaction (Mindlin & Deresewicz, 1953)

basic principles
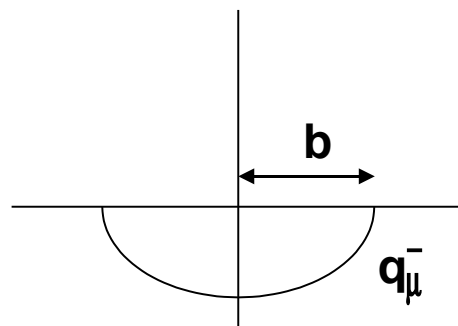

$$p = \left(\frac{3N}{2\pi a^2} \right) (a^2 - r^2)^{1/2}$$

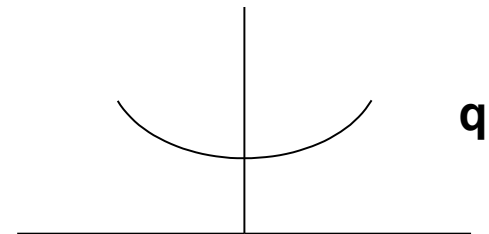$$q_\mu^+ = \left(\frac{3\mu N}{2\pi a^2} \right) (a^2 - r^2)^{1/2}$$

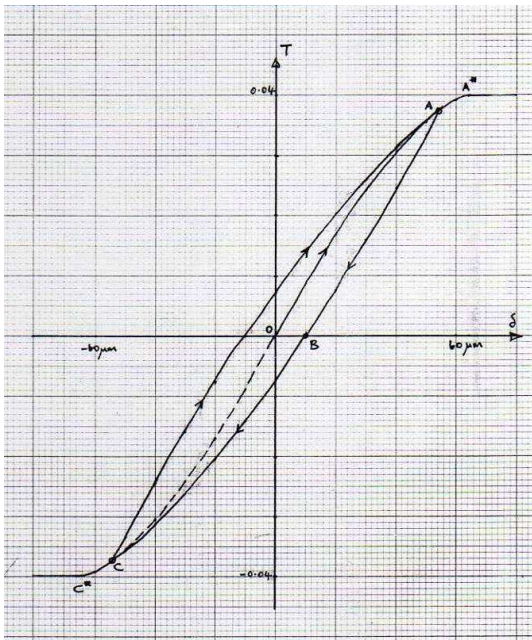$$q_\mu^- = - \left(\frac{3\mu N}{2\pi a^3} \right) (b^2 - r^2)^{1/2}$$

$$q = \left(\frac{3\mu N}{2\pi a^3} \right) (a^2 - r^2)^{1/2} \text{ for } b \leq r \leq a$$

$$q = \left(\frac{3\mu N}{2\pi a^3} \right) \left[(a^2 - r^2)^{1/2} - (b^2 - r^2)^{1/2} \right] \text{ for } 0 \leq r \leq b$$
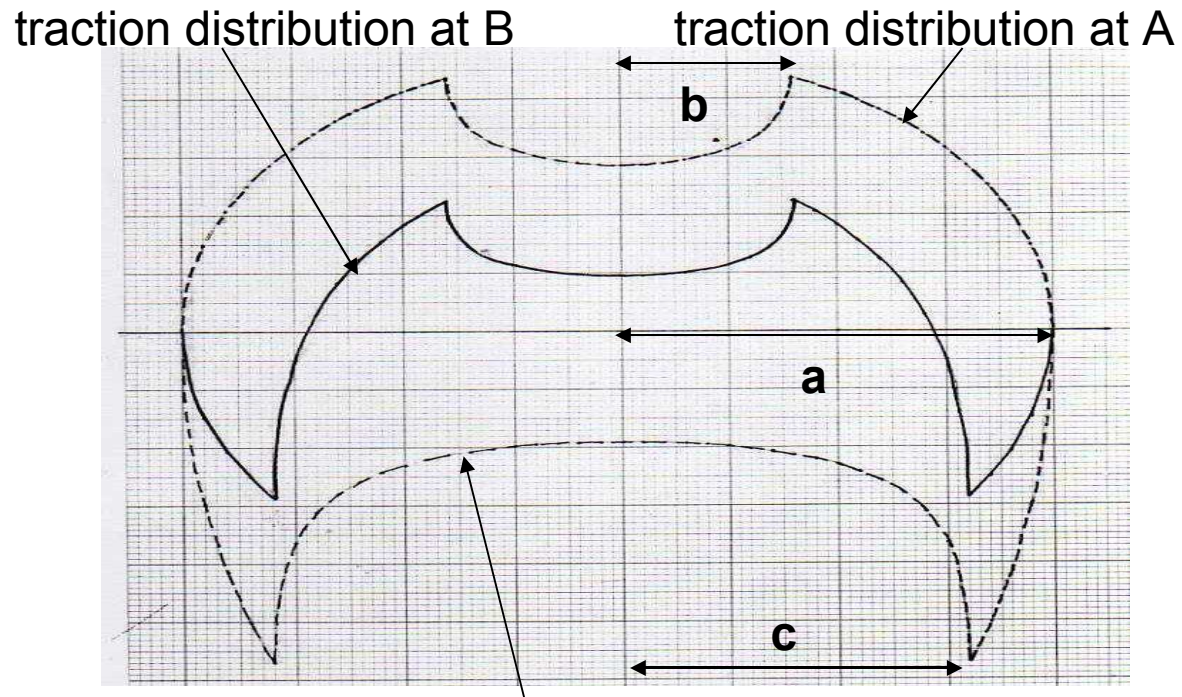
traction distribution at B   traction distribution at A

force-displacement   traction distribution due to unloading from A to B

loading – O to A

unloading – A to C

$$q = -\left(\frac{3\mu N}{2\pi a^3}\right)\left(a^2 - r^2\right)^{1/2} \qquad\qquad c \le r \le a$$

reloading – C to A

inverse loading – C to C*

$$q = \left(\frac{3\mu N}{2\mu a}\right)\left[\left(a^2 - r^2\right)^{1/2} - 2\left(c^2 - r^2\right)^{1/2}\right] \qquad b \le r \le c$$

$$q = \left(\frac{3\mu N}{2\pi a}\right)\left[\left(a^2 - r^2\right)^{1/2} - \left(b^2 - r^2\right)^{1/2} - 2\left(c^2 - r^2\right)^{1/2}\right] \qquad 0 \le r \le b$$

$$\Delta \delta = \frac{1}{8G^{*}a}\left[\pm \mu \Delta N + \frac{\Delta T \mp \mu \Delta N}{\theta}\right]$$

$$\Delta \delta = \Delta \delta_{1} + \Delta \delta_{2}$$
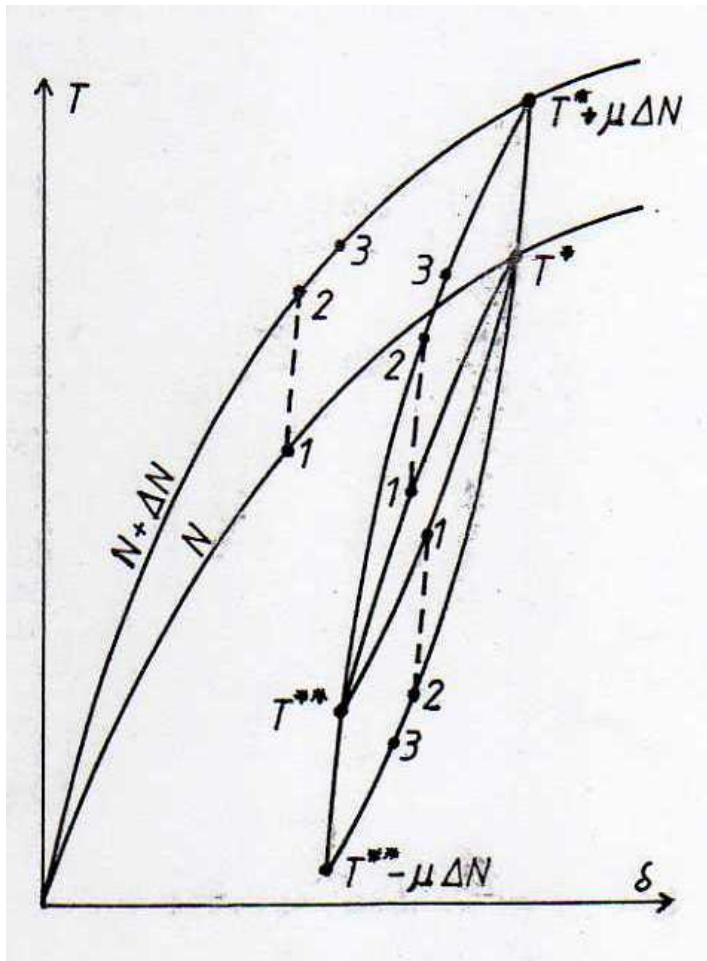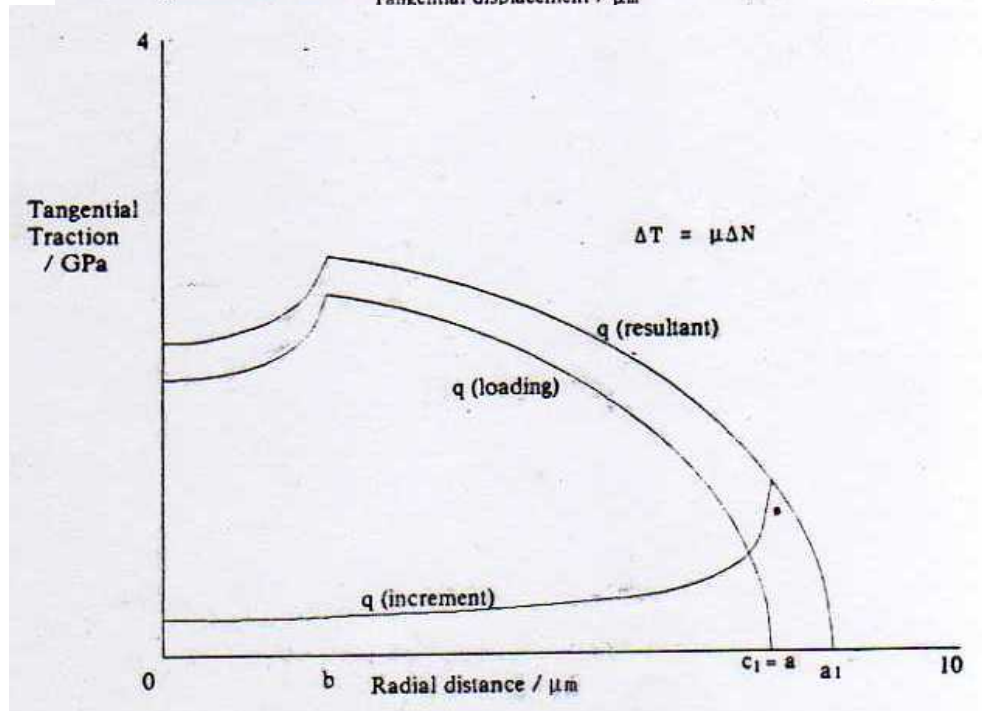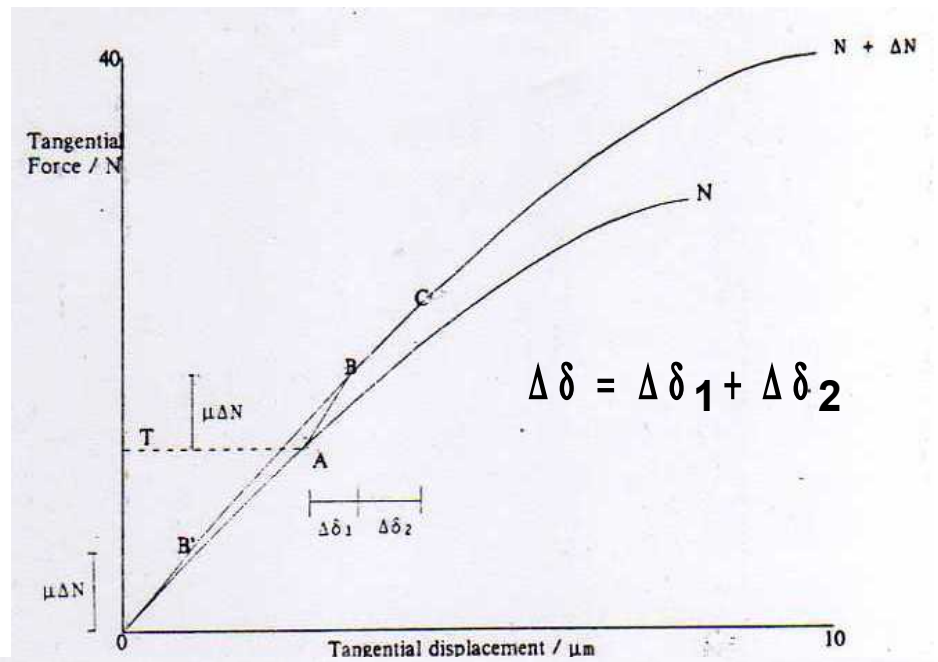
DEM implementation   Thornton & Randall (1988)

see also Thornton (1999) Mechanics of granular materials – an introduction.
(Oda & Iwashita, eds.) Balkema, 207-217.

$$k_t = \frac{\Delta T}{\Delta \delta} = 8G^* a\theta \pm \mu(1-\theta)\frac{\Delta N}{\Delta \delta}$$

negative sign only invoked during unloading

$$\theta^3 = 1 - \frac{(T + \mu \Delta N)}{\mu N} \qquad \Delta \delta > 0 \qquad \text{(loading)}$$

$$\theta^3 = 1 - \frac{(T^* - T + 2\mu \Delta N)}{2\mu N} \qquad \Delta \delta < 0 \qquad \text{(unloading)}$$

$$\theta^3 = 1 - \frac{(T - T^* + 2\mu \Delta N)}{2\mu N} \qquad \Delta \delta > 0 \qquad \text{(reloading)}$$

except when $\Delta N > 0$ and $\Delta \delta < \dfrac{\mu \Delta N}{8G^* a}$ i.e. $\Delta T < \mu \Delta N$ in which case $\theta = 1$

and $\theta = 1$ until $\sum \Delta T \geq \mu \sum \Delta N$

FEM simulations   Wu (2001)

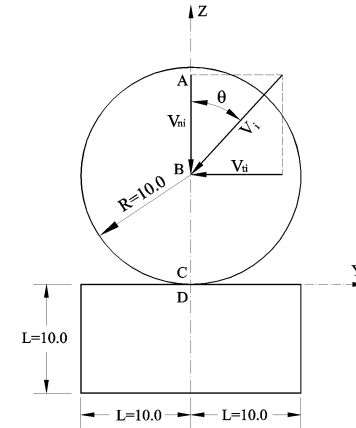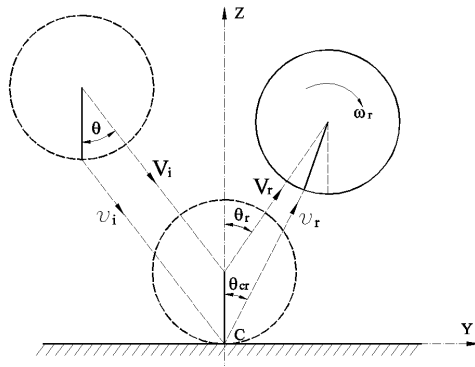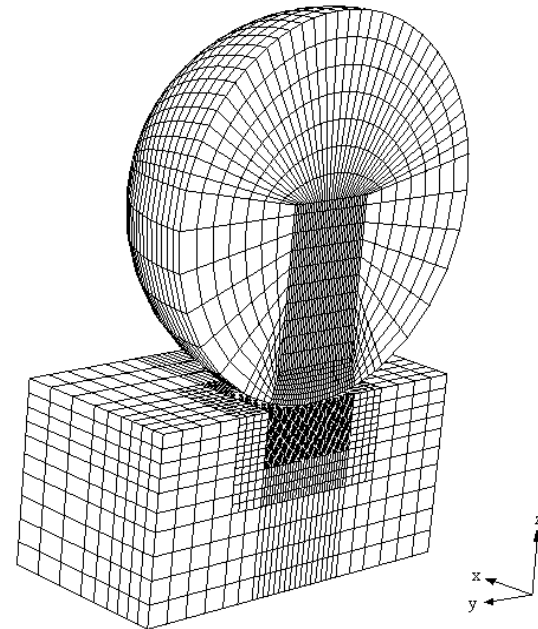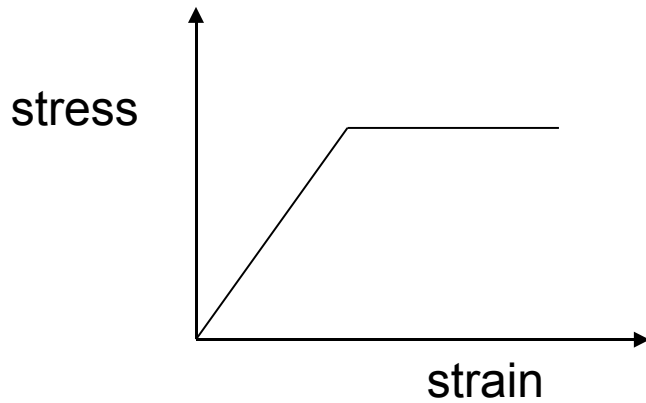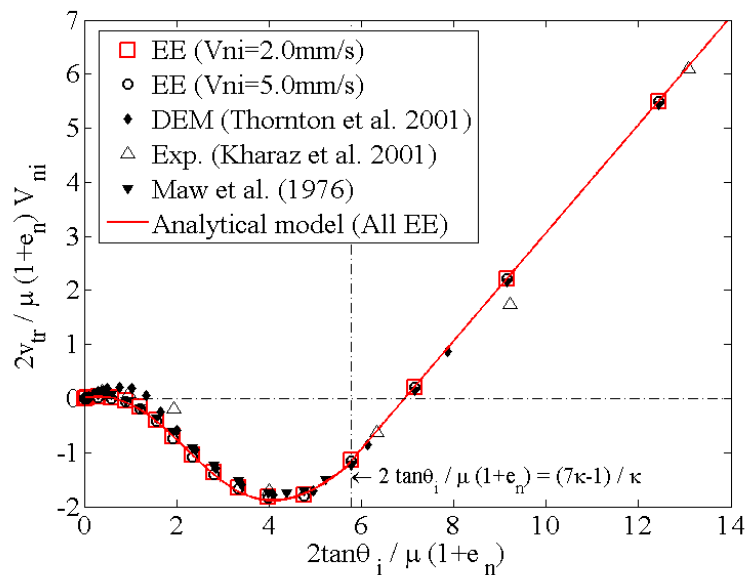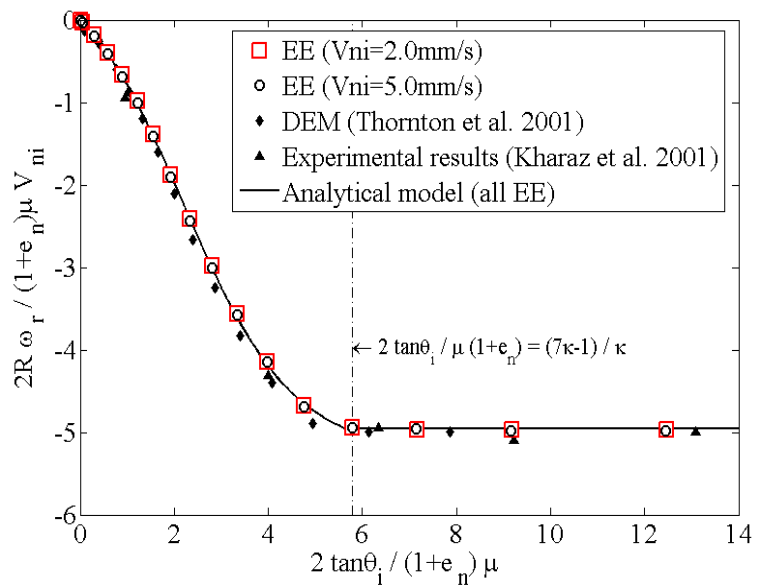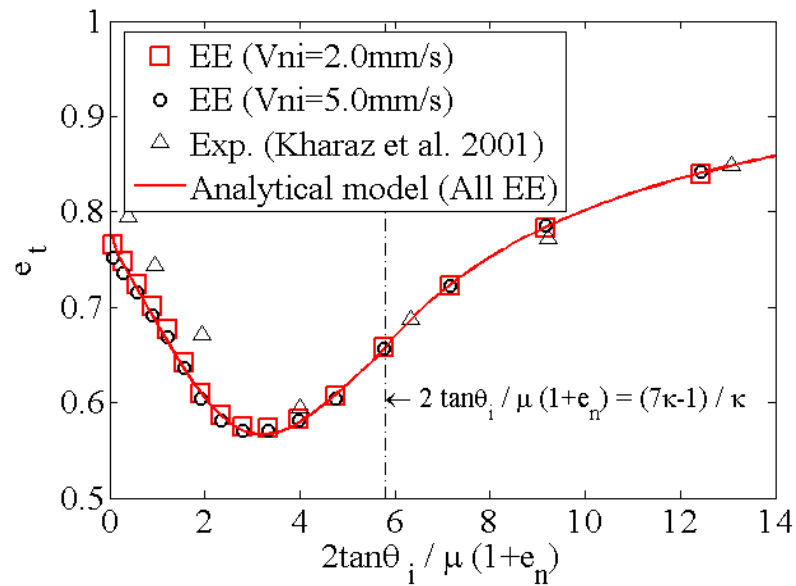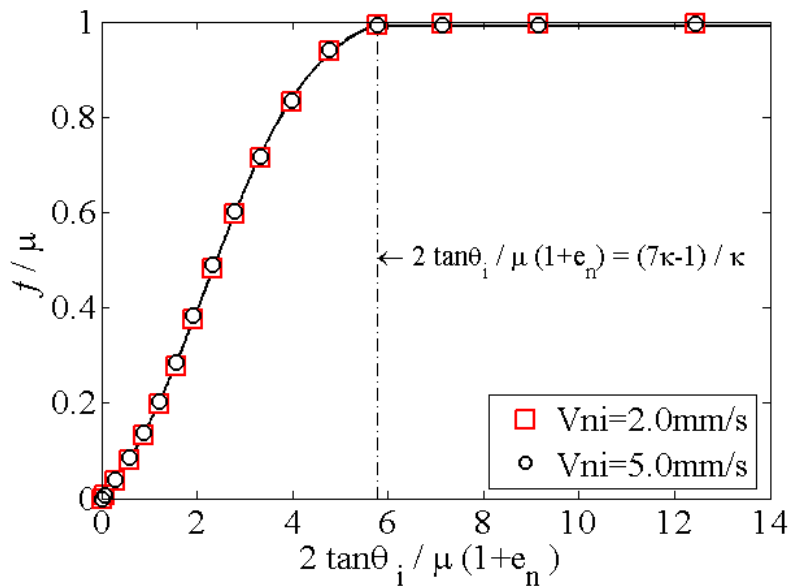Diagram of the oblique impact of a sphere with a plane surface.

stress

strain

FE model for the oblique impact of a sphere with a half-space

Top-left plot: f/μ versus $2\tan\theta_i / \mu (1+e_n)$. Annotation: $\leftarrow 2\tan\theta_i / \mu (1+e_n) = (7\kappa-1)/\kappa$. Legend: Vni=2.0mm/s (red square), Vni=5.0mm/s (circle).

Top-right plot: e_t versus $2\tan\theta_i / \mu (1+e_n)$. Legend: EE (Vni=2.0mm/s) (red square), EE (Vni=5.0mm/s) (circle), Exp. (Kharaz et al. 2001) (triangle), Analytical model (All EE) (red line). Annotation: $\leftarrow 2\tan\theta_i / \mu (1+e_n) = (7\kappa-1)/\kappa$.

Bottom-left plot: $2R\omega_r / (1+e_n)\mu V_{ni}$ versus $2\tan\theta_i / (1+e_n)\mu$. Legend: EE (Vni=2.0mm/s), EE (Vni=5.0mm/s), DEM (Thornton et al. 2001), Experimental results (Kharaz et al. 2001), Analytical model (all EE). Annotation: $\leftarrow 2\tan\theta_i / \mu (1+e_n) = (7\kappa-1)/\kappa$.

Bottom-right plot: $2v_{tr} / \mu (1+e_n) V_{ni}$ versus $2\tan\theta_i / \mu (1+e_n)$. Legend: EE (Vni=2.0mm/s), EE (Vni=5.0mm/s), DEM (Thornton et al. 2001), Exp. (Kharaz et al. 2001), Maw et al. (1976), Analytical model (All EE). Annotation: $\leftarrow 2\tan\theta_i / \mu (1+e_n) = (7\kappa-1)/\kappa$.
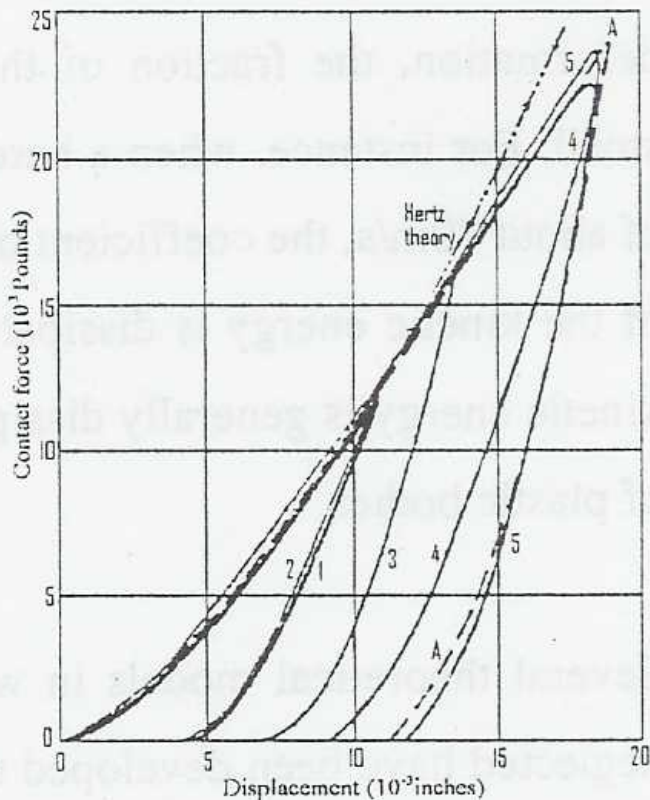
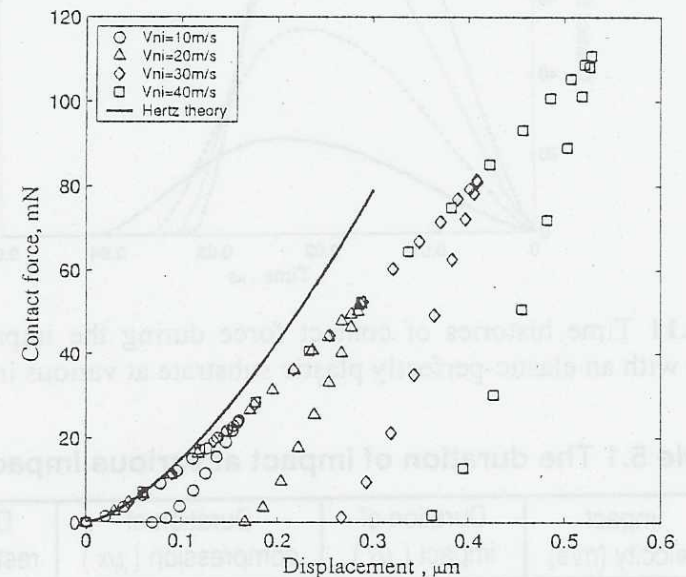# ELASTIC-PERFECTLY PLASTIC CONTACT INTERACTIONS

Normal interaction

If plastic deformation occurs then the applied displacement is not fully recovered and the loading and unloading curves do not coincide.

Force-displacement curves for elastoplastic impact experiments

(Goldsmith & Lyman, 1960)


FEM results (Thornton et al, 2001)

Contact pressure distributions during loading

As shown in the figure, the Hertzian pressure distribution is valid until the pressure at the centre of the contact is equal to 1.6 times the yield stress of the material, at which point yield occurs below the centre of the contact area. Further compression results in a spreading of the plastic deformation zone below the surface and a slight modification of the shape of the contact pressure distribution as the maximum contact pressure increases further. When the pressure at the centre of the contact reaches about 2.4 times the yield stress the plastic deformation zone in the substrate reaches the contact surface at the perimeter of the contact area. Beyond this point, further compression results in a significant change in the form of the pressure distribution. Over an increasing central portion of the contact area the contact pressure becomes almost constant with only a small increase in the pressure at the centre of the contact.

Li, Wu & Thornton (2002) presented a theoretical model, which considered the variation of the maximum pressure with compression and the change in the contact curvature owing to irrecoverable plastic deformation during loading. They obtained theoretical force displacement predictions in very good agreement with the FEM data. However, no tangible analytical solution is available.

FEM results (Wu, Li & Thornton, 2003)
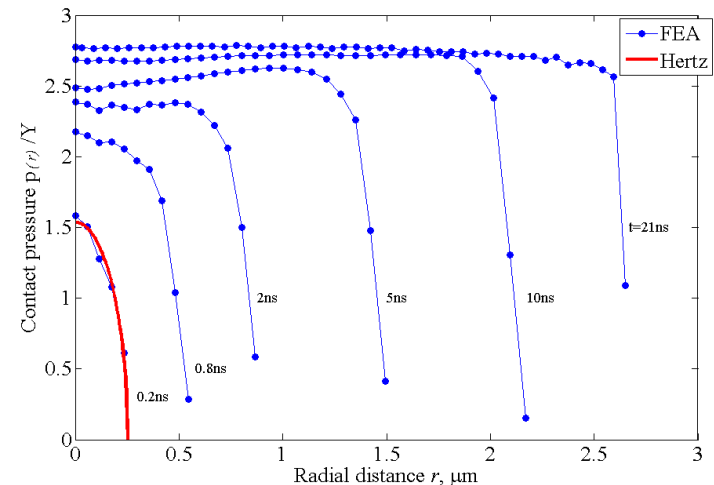
# Contact pressure distributions during unloading

Although the unloading is elastic, as can be seen from the figure, the pressure distributions are not Hertzian.

The problem has been solved by Mesarovic and Johnson (2000) who derived the following expression for the pressure distribution

$$p = \frac{2p^*}{\pi} \sin^{-1}\left(\frac{a^2 - r^2}{a^{*2} - r^2}\right)^{1/2} \quad \text{where} \quad p^* \text{ and } a^*$$

are the pressure and contact radius at the start of unloading.

Unfortunately the theory does not lead to an analytical solution for the contact force-displacement curve.
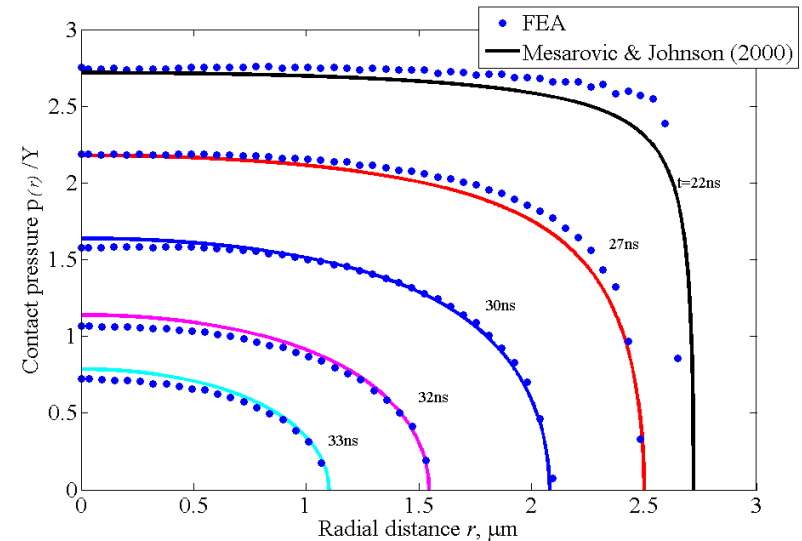
FEM results (Wu, Li & Thornton, 2003)

A simplified analytical solution

A limiting contact pressure p_y is defined and it is assumed that **for $p_0 \leq p_y$ the response is elastic.**

It is also assumed that further compression results in fully plastic deformation.

Figure 1. (a) Normal traction distribution for an elastic–perfectly plastic sphere under loading. (b) Corresponding force–displacement relationships.

In order to model the plastic phase the normal contact pressure distribution is approximated by a Hertzian distribution with a cut-off defined by the limiting contact pressure, as shown in the figure.

Thornton (1997), Thornton & Ning (1998), Mishra & Thornton (2002)

The consequence of this is that the plastic loading curve is given by a straight line tangent to the Hertzian curve at $\left(N_y, \alpha_y\right)$

$$N = N_y + \pi\, p_y R^* \left(\alpha - \alpha_y\right)$$

$$N_y = 2\left(N^* - k_p \alpha^*\right)$$

$$k_p = \pi R^* p_y$$

The limiting contact pressure can be considered to be an approximation to the hardness, which is related to the yield stress σ_y by a constraint factor c.
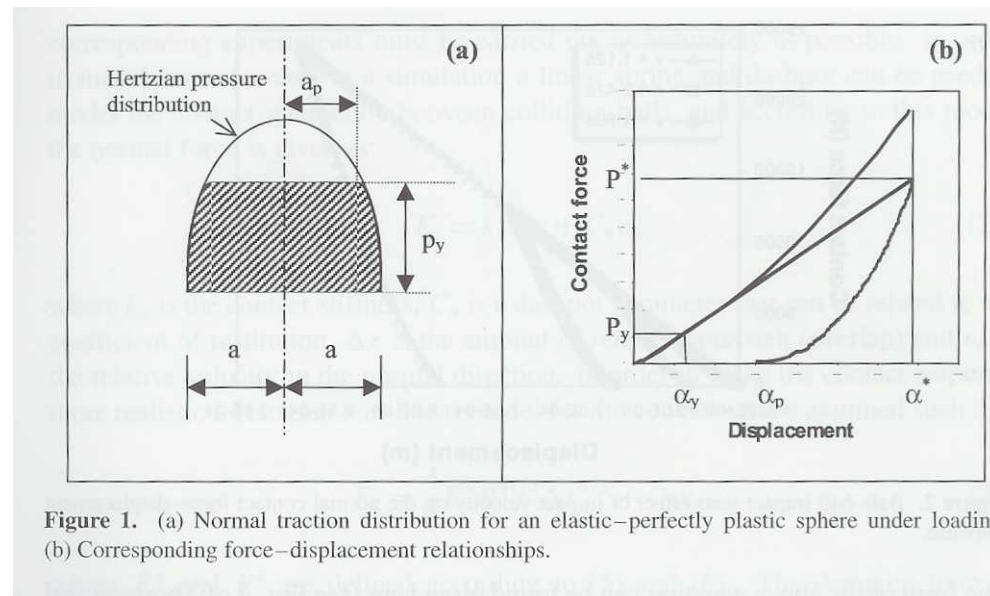
$$p_y = c\sigma_y \quad \text{with} \quad 2.4 \leq c \leq 3.0$$
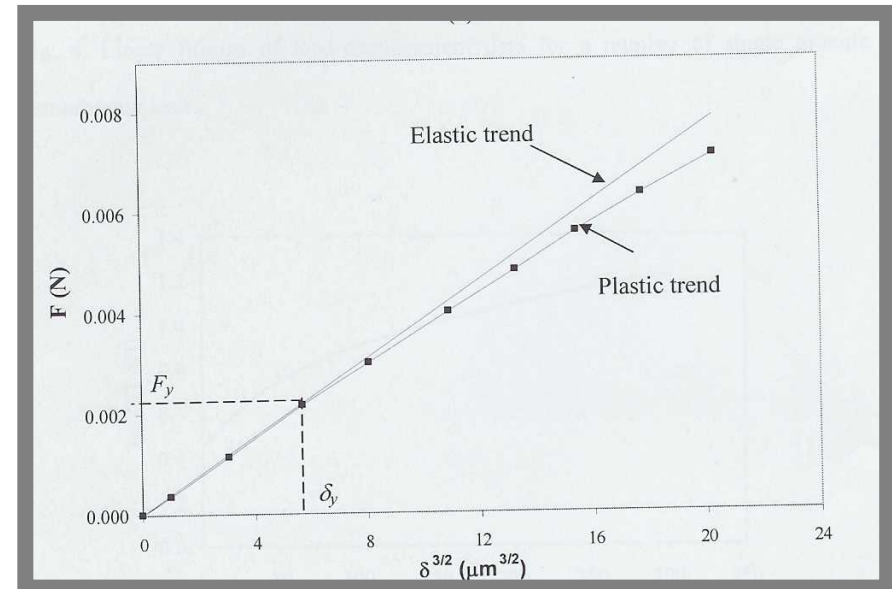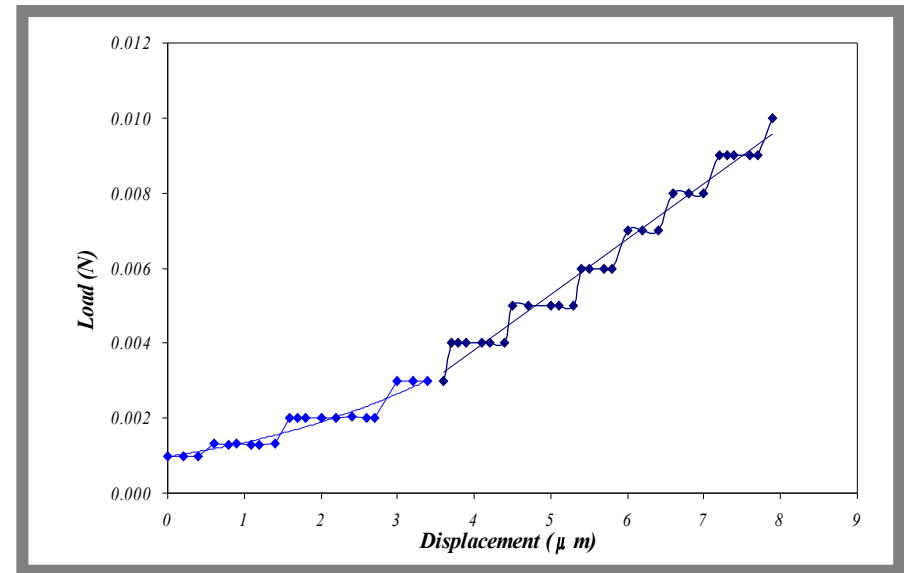
Application   Samini (2003)

Diametrical compression tests
(using an Instron testing machine
with a 10 N load cell) on 'spherical'
soft synthetic detergent granules.

Plot **N** against $\alpha^{3/2}$

Fit straight line to data points

for $N < N_y$ to obtain slope **K**.

$$E = \frac{3\left(1 - \nu^2\right)K}{4\sqrt{R}}$$

Samini, Hassanpour & Ghadiri (2005)

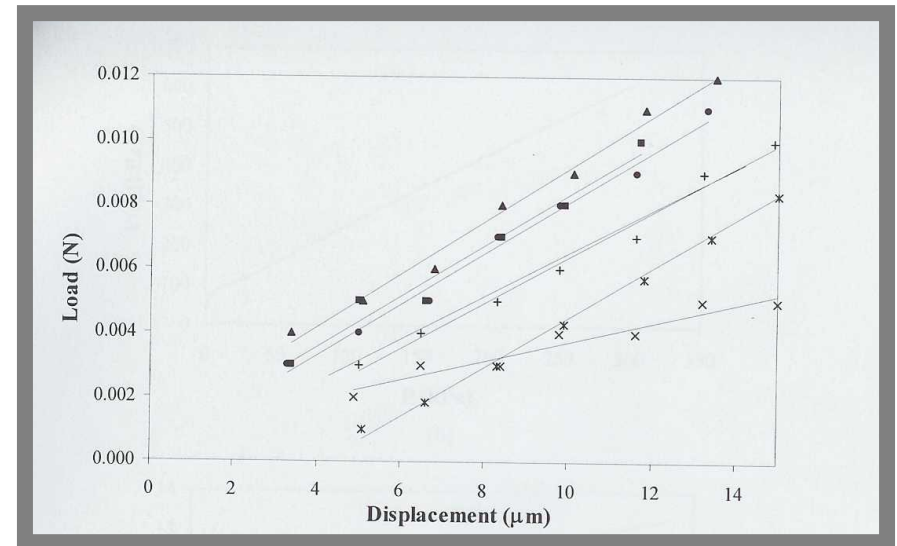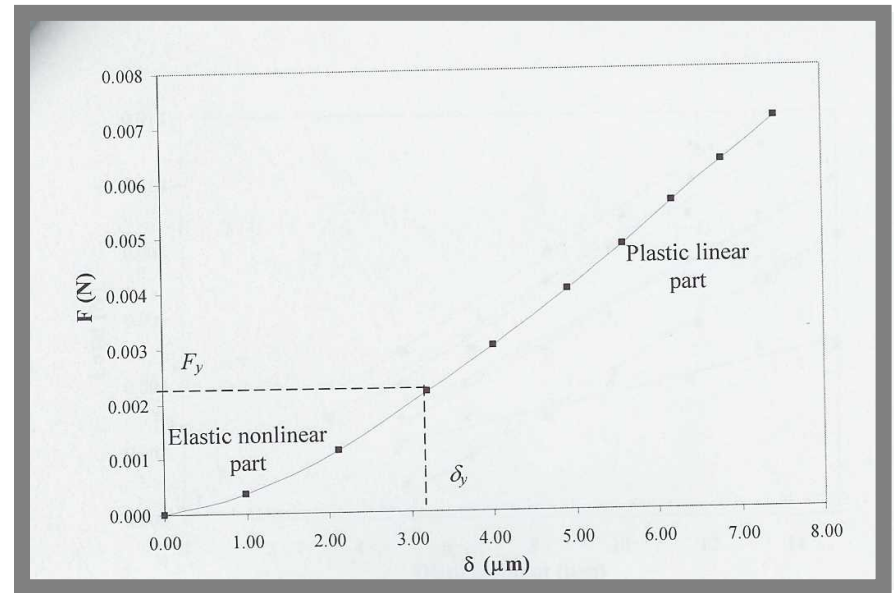On a plot of **N** against α

Fit straight line to data points

for **N** > **N$_y$** to obtain slope **k$_p$**

Calculate limiting contact pressure and yield stress.

$$p_y = \frac{k_p}{\pi R^*} \quad \text{and} \quad \sigma_y = \frac{p_y}{c}$$

Size (mm)	σ_y (kPa)	E (MPa)
1.70-2.00	297 $\pm$108	7.5 $\pm$3
1.00-1.18	405 $\pm$151	10 $\pm$5

(assumes **p$_y$ = 3σ$_y$**)

Samini, Hassanpour & Ghadiri (2005)

comments

Both the FEM results of Wu et al (2003)
and the Thornton (1997) approximation
only strictly apply to linear elastic-
perfectly plastic material, as illustrated by
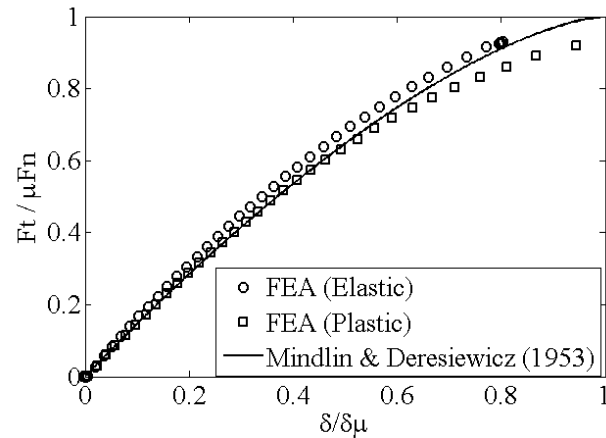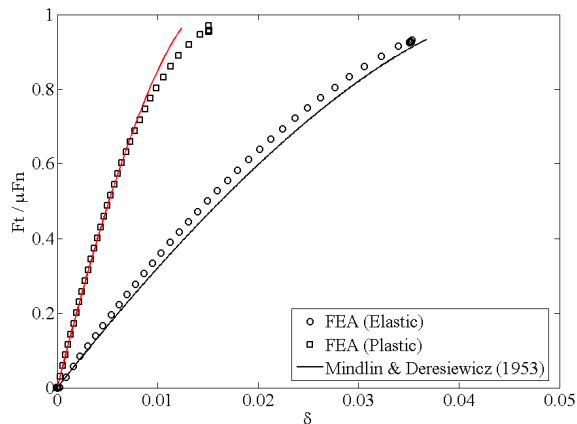the stress-strain curve shown in the figure.
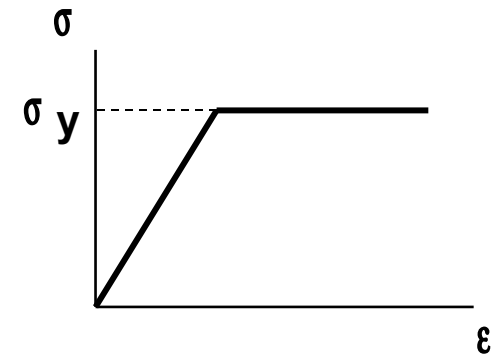
Many materials exhibit strain hardening and, for most materials, the
measurement of the so-called yield stress is ambiguous. Therefore one should
be somewhat circumspect with regard to values of yield stress provided by
the manufacturer.

If one wishes to estimate the yield stress from the limiting contact
pressure then one must select an appropriate constraint factor for the
level of loading applied.

Tangential interaction

FEM simulations have shown that the theory of Mindlin & Deresiewicz (1953) applies to both elastic and elastoplastic particles, Wu & Thornton (2007).
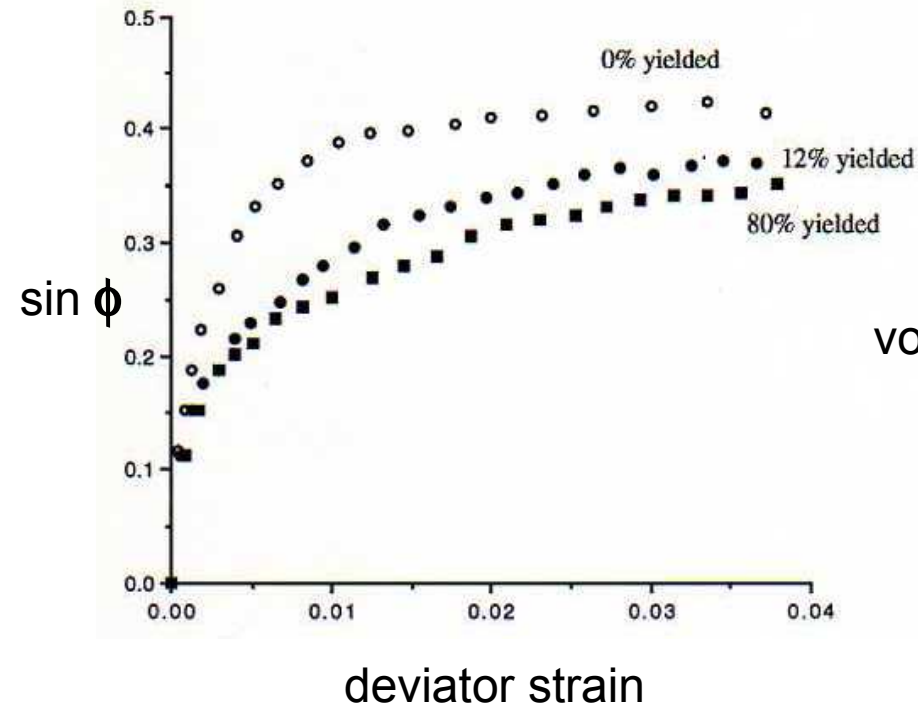

$$T = \mu N \left[1 - \left(1 - \frac{\delta}{\delta_\mu} \right)^{3/2} \right] \quad \text{where} \quad \delta_\mu = \frac{3\mu N}{16 G^* a}$$

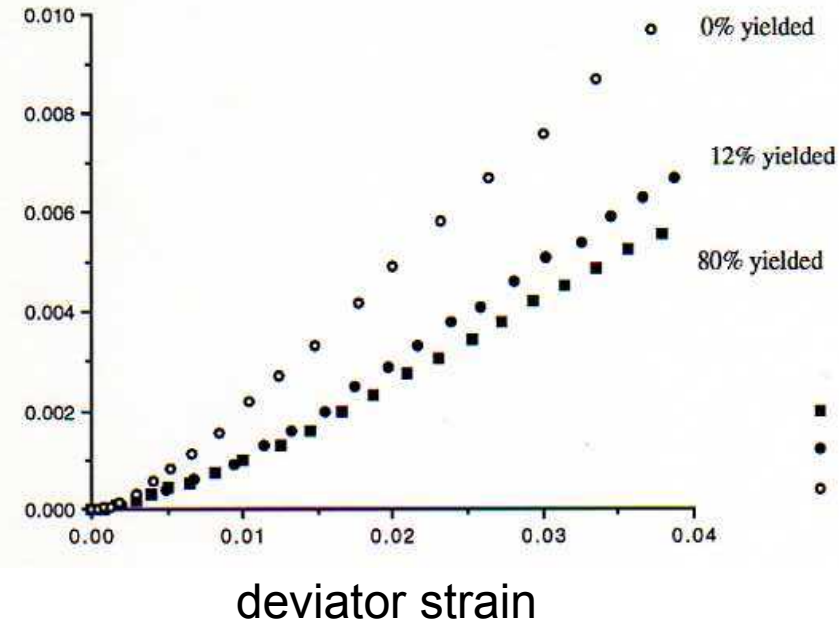$$\frac{1}{G^*} = \frac{(2 - \nu_1)}{G_1} + \frac{(2 - \nu_2)}{G_2}$$

$$G_i = \frac{E_i}{2(1 + \nu_i)}$$

Effect of contact plastic deformation
on the quasi-static stress-strain – dilation response

axisymmetric compression in a periodic cell

Thornton (2000)

AUTOADHESIVE CONTACT INTERACTIONS (ELASTIC)

In particle technology there is an increasing desire to have smaller and smaller particles. For particle sizes less than say 50 μm, van der Waals forces become significant and particles tend to stick to each other.

Two theoretical models for the autoadhesion of spheres were developed over 30 years ago (a) the JKR model (Johnson, Kendall & Roberts, 1971) and (b) the DMT model (Derjaguin, Muller & Topolov, 1975).

The two models were initially thought to be competitive but subsequently shown to be limits to a range of solutions (Maugis, 1992) that are governed by the non-dimensional parameter

$$\mu = \left(\frac{R\Gamma^2}{E^{*2} z_0^3} \right)^{1/3}$$

where z_0^3 is the equilibrium separation in the Lennard-Jones potential.

For like bodies, the interface energy is twice the surface energy, $\Gamma = 2\gamma$.

It is now common practice to use the atomic force microscope (AFM) to measure the 'pull-off' force necessary to break an autoadhesive contact and deduce the surface energy. The interpretation depends on the model used.

DMT theory is appropriate for $\mu \leq$ **0.1** and the pull-off force $N_c = 2\pi \Gamma R^*$

JKR theory is appropriate for $\mu \geq$ **5** and the pull-off force $N_c = 1.5\pi \Gamma R^*$

For intermediate values of μ see Maugis (1992) – very complicated.

Note that, in both the DMT and JKR models, the pull-off force is independent of the elasticity of the particles.

Assume the JKR model of adhesion
Johnson, Kendall & Roberts (1971)

Johnson (1976) gives the normalised
force-displacement equation as

Fig. 5. Force–displacement relationship for adhesive elastic spheres.

$$\frac{\alpha}{\alpha_f} = \frac{3\left(\dfrac{N}{N_c}\right) + 2 \pm 2\left(1 + \dfrac{N}{N_c}\right)^{1/2}}{3^{2/3}\left[\dfrac{N}{N_c} + 2 \pm 2\left(1 + \dfrac{N}{N_c}\right)^{1/2}\right]^{1/3}}$$

where the pull-off force $\boxed{N_c = \dfrac{3}{2}\pi\,\Gamma\,R^*}$

and $\qquad \alpha_f = \dfrac{3}{4}\left(\dfrac{\pi^2\Gamma^2 R^*}{E^{*2}}\right)^{1/3} = \left(\dfrac{3N_c^2}{16R^*E^{*2}}\right)^{1/3}$

Alternatively, from Johnson (1985)

$$N = \frac{4E^*a^3}{3R^*} - 4\left(\frac{\pi \Gamma E^* a^3}{2}\right)^{1/2} \qquad \alpha = \frac{a^2}{R^*} - 2\left(\frac{\Gamma \pi a}{2E^*}\right)$$

therefore

$$\frac{dN}{da} = \frac{4E^* a^2}{R^*} - 6\left(\frac{\pi \Gamma E^* a}{2}\right)^{1/2} \qquad \frac{d\alpha}{da} = \frac{2a}{R^*} - \left(\frac{\pi \Gamma}{2E^* a}\right)^{1/2}$$

$$\frac{dN}{d\alpha} = \frac{4E^{*2} a^3 - 6\left(\frac{\pi \Gamma R^{*2} E^{*3} a^3}{2}\right)^{1/2}}{2E^* a^2 - \left(\frac{\pi \Gamma R^{*2} E^* a}{2}\right)^{1/2}} \qquad \text{or} \qquad \boxed{k_n = 2E^* a\left[\frac{3 - 3\sqrt{N_c / N'}}{3 - \sqrt{N_c / N'}}\right]}$$

in which **N'** is the Hertzian force necessary to create the same contact area.

$$\boxed{N' = N + N_c + \sqrt{4NN_c + 4N_c^2}} \qquad \text{and} \qquad \boxed{a = \left(\frac{3N'R^*}{4E^*}\right)^{1/3}}$$

AUTOADHESIVE ELASTOPLASTIC SPHERES

If the interaction is not elastic then the unloading curves and the pull-off force depend on the magnitude of the force from which unloading commenced, as illustrated in the figure.

The figure shows a numerical solution obtained using DEM.

There is no analytical solution.

It may be possible, using a DEM code with the appropriate contact mechanics algorithms, to match experimental data.

Fig. 8. Effect of impact velocity on the normal contact force–displacement response for adhesive, elastic–perfectly plastic spheres.
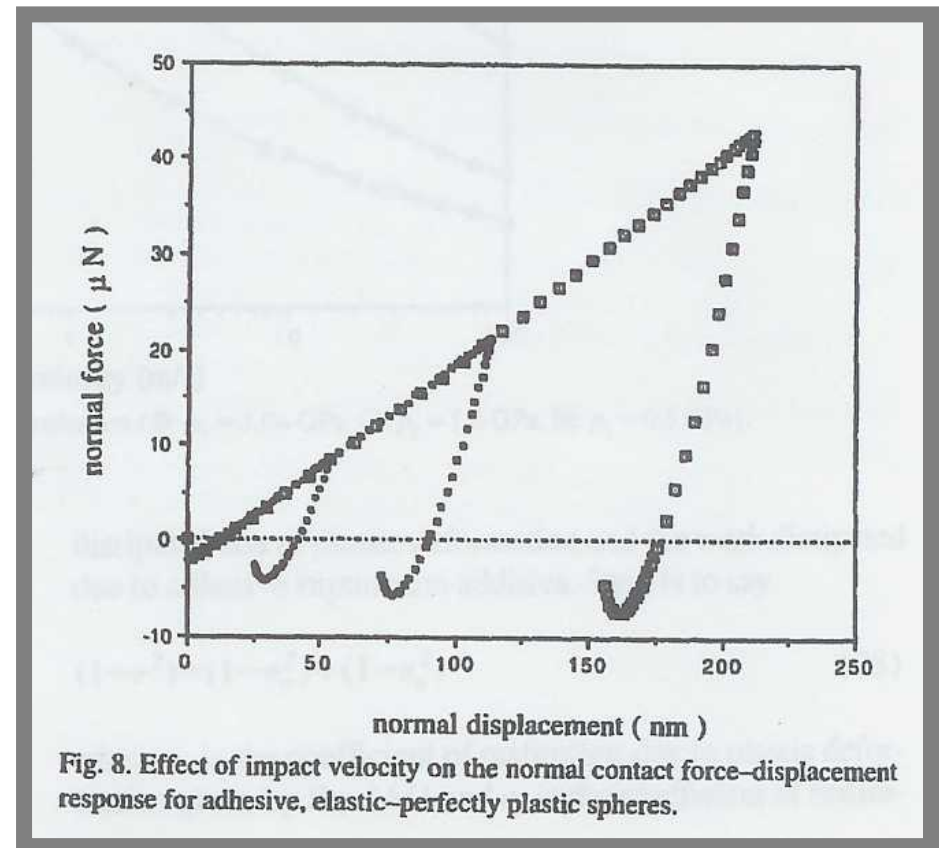
Thornton & Ning (1998)

Tangential interactions for autoadhesive systems

Thornton (1991),Thornton & Yin (1991)

Savkoor & Briggs (1977) extended JKR theory to the initial application of a tangential force and showed that the contact radius is then defined by

$$a^3 = \frac{3R^*}{4E^*}\left[N + 2N_c \pm \left(4NN_c + 4N_c^2 - \frac{T^2E^*}{4G^*}\right)^{1/2}\right]$$

until

$$T_{crit} = 4\left[\frac{G^*}{E^*}\left(NN_c + N_c^2\right)\right]^{1/2}$$

The above describes a peeling mechanism, during which $k_t = 8G^*a$

Mindlin (1949)

If $T > T_{crit}$ revert to Mindlin & Deresiewicz (1953).

The problem is not yet resolved.

see Johnson (1997)

AGGLOMERATE-AGGLOMERATE COLLISIONS   Kafui & Thornton (1996)

initial state
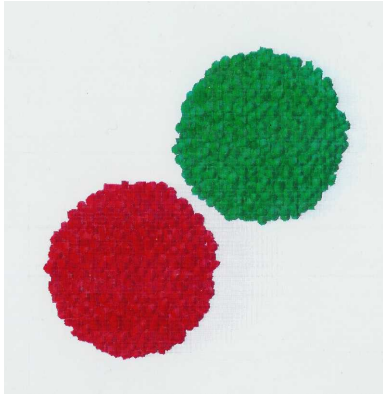
Each agglomerate has 2000 primary particles of average size 100 microns.

Relative impact speed is 1 m/s.

Surface energy is 1 J/m^2.

different impact angles θ

θ = **45°**

θ = **0°**

θ = **15°**
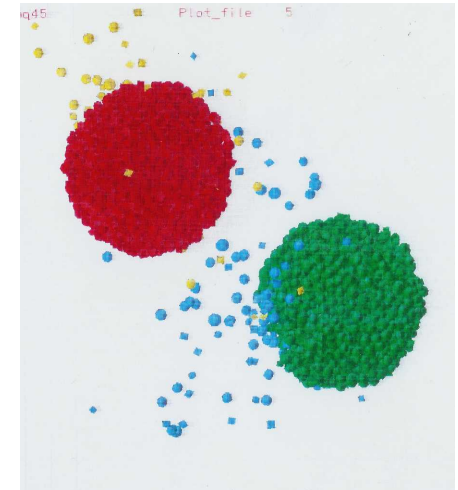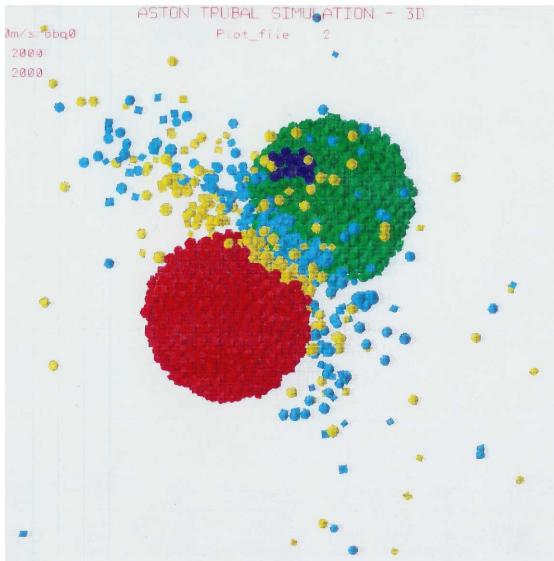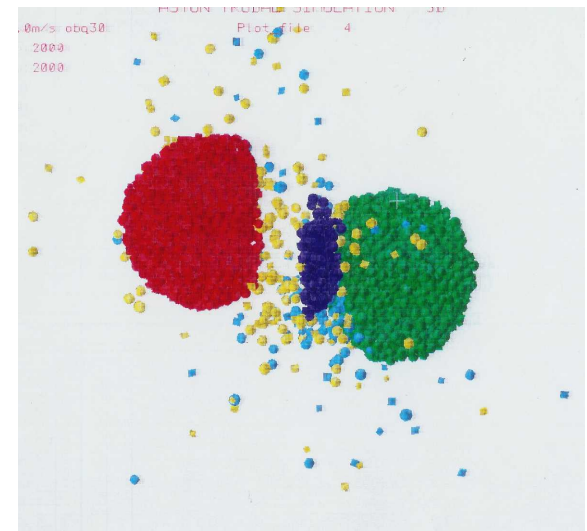
θ = **30°**

The effect of surface energy on the transition from fixed bed to bubbling bed
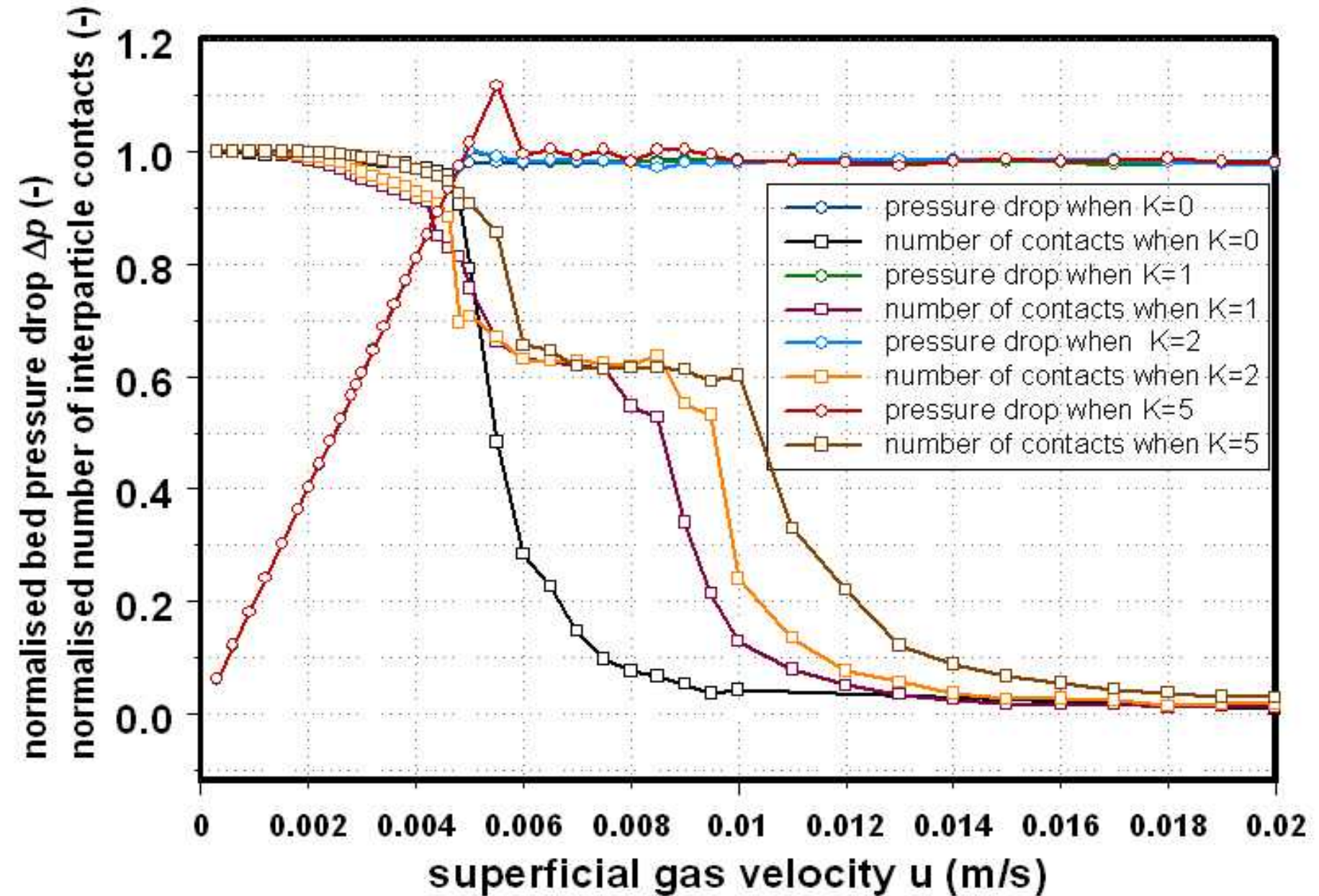
SNAPSHOTS OF CLUSTER DEGRADATION WITH INCREASE OF SUPERFICIAL GAS VELOCITY

❏ In each snapshot below, the three columns (from left to right) represent: the six largest clusters in the system, singlets, doublets and triplets and the connectivity network.
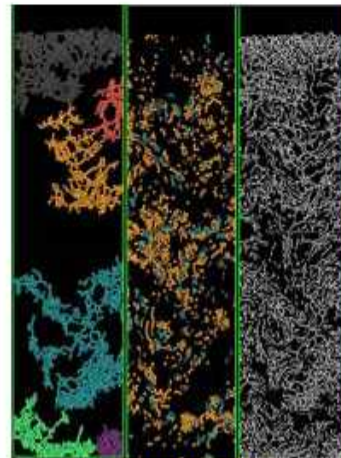
Interparticle pull-off force = 0
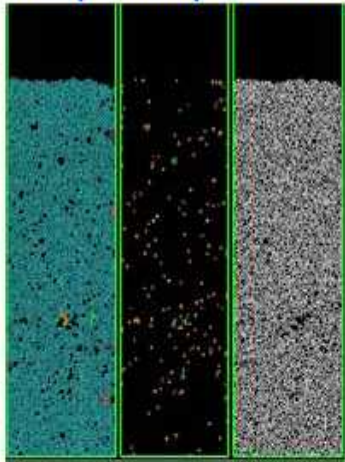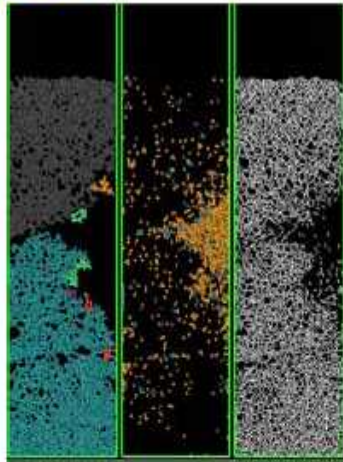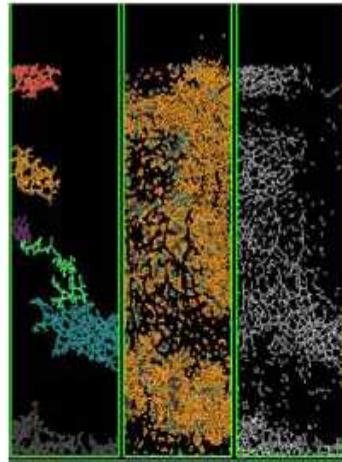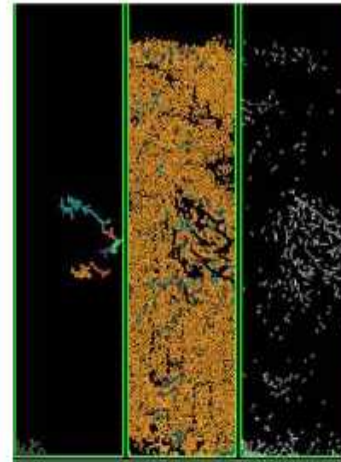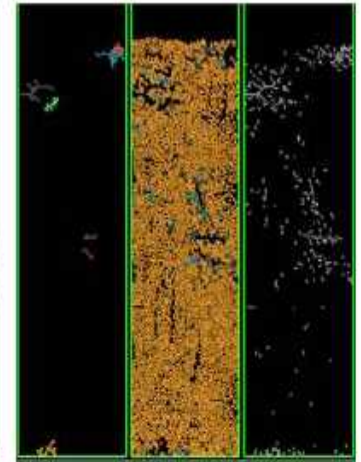
| U = 0.0048 m/s | U = 0.0050 m/s | U = 0.0060 m/s | U = 0.0080 m/s | U = 0.0085 m/s |

Interparticle pull-off force = <mg> (K = 1)
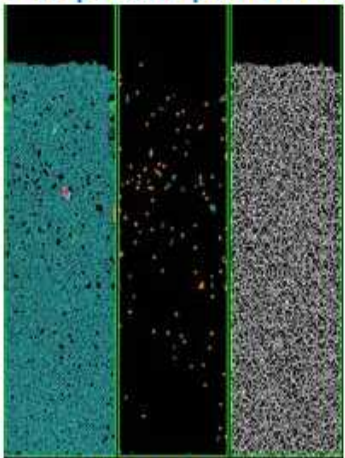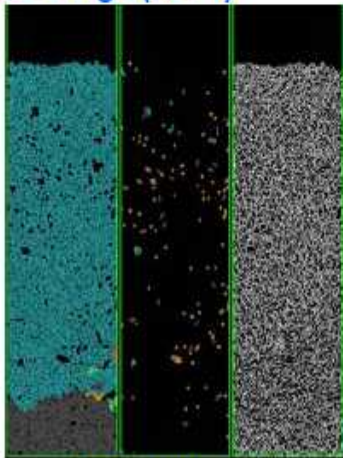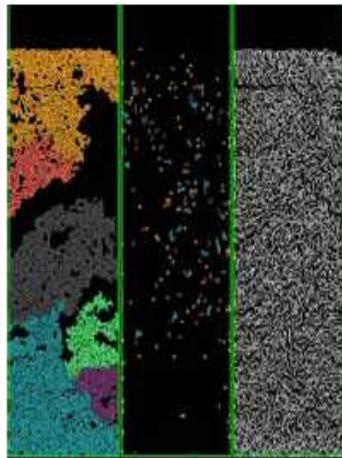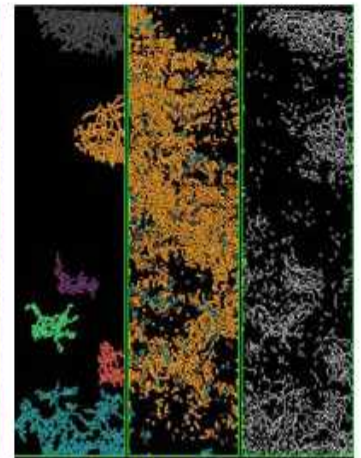
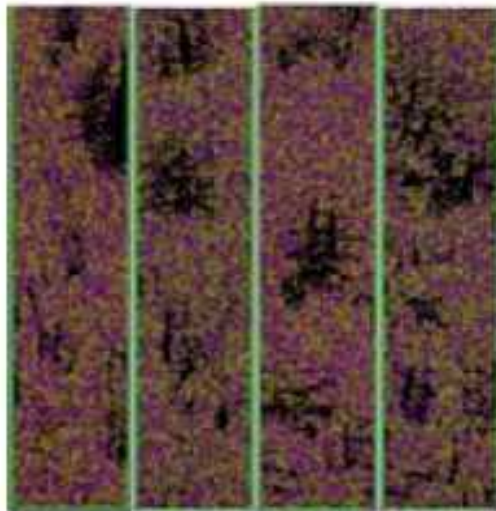| U = 0.0048 m/s | U = 0.0050 m/s | U = 0.0060 m/s | U = 0.0080 m/s | U = 0.0095 m/s |

U = 0.02 m/s
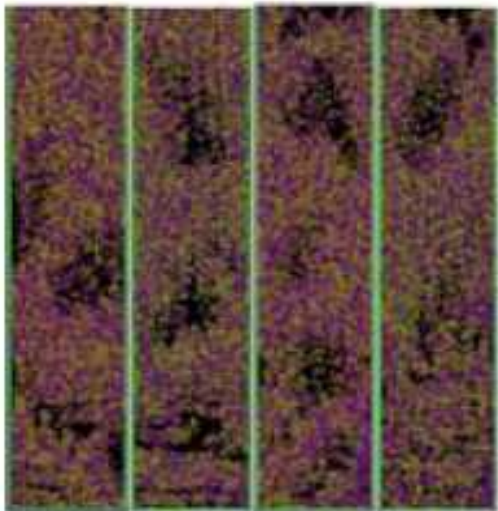
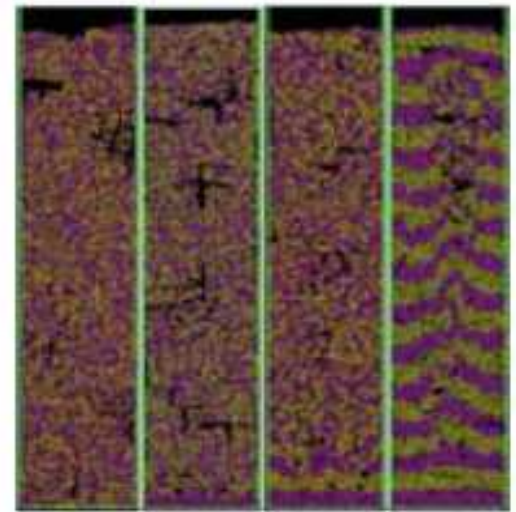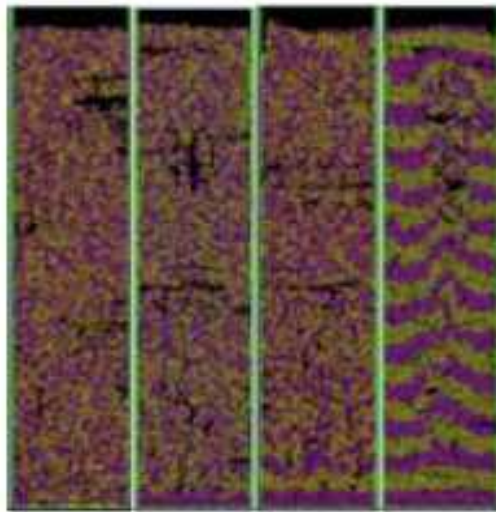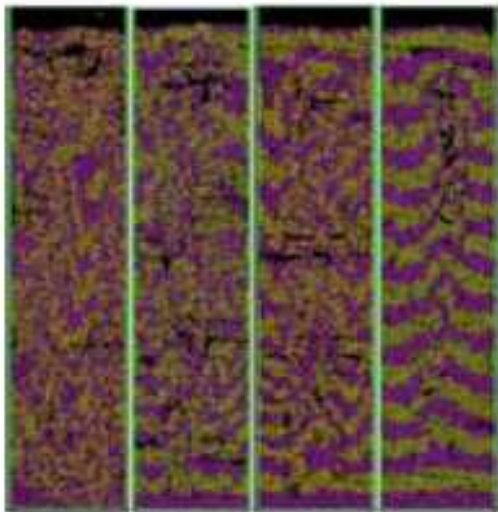K = 0 K = 1 K = 2 K = 5   K = 0 K = 1 K = 2 K = 5   K = 0 K = 1 K = 2 K = 5
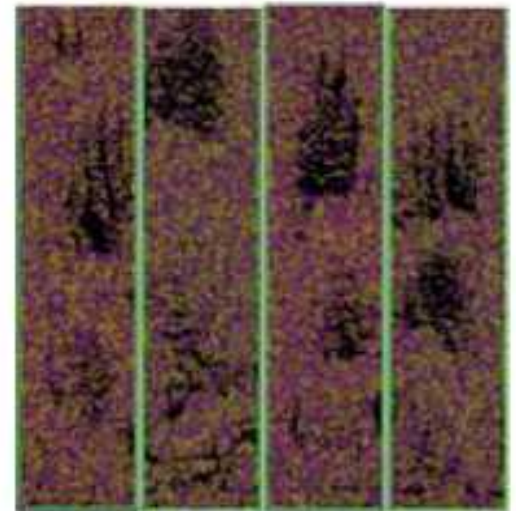
U = 0.01 m/s

Time

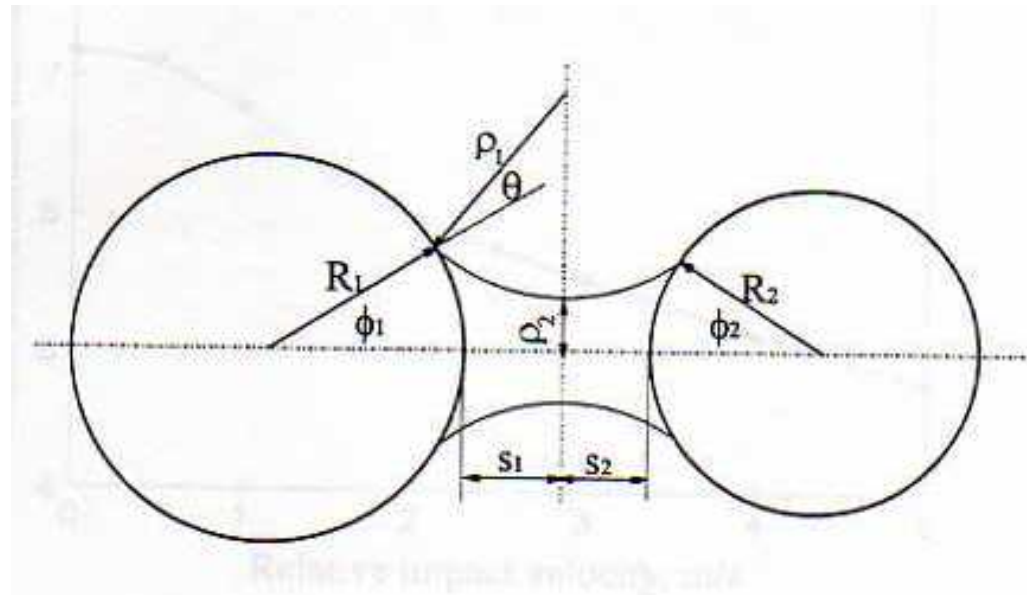Note that in the homogeneous expansion regime, U = 0.01 m/s, channelling occurs when K = 5

Liquid bridges (pendular)

Lian, Thornton & Adams (1993)

Toroidal approximation

Fisher (1926)

$$\rho_1 = \frac{S_1 + R_1(1 - \cos\phi_1)}{\cos(\phi_1 + \theta)} = \frac{S_2 + R_2(1 - \cos\phi_2)}{\cos(\phi_2 + \theta)}$$

$$\rho_2 = R_1 \sin\phi_1 - \frac{[1 - \sin(\phi_1 + \theta)][S_1 + R_1(1 - \cos\phi_1)]}{\cos(\phi_1 + \theta)}$$

$$= R_2 \sin\phi_2 - \frac{[1 - \sin(\phi_2 + \theta)][S_2 + R_2(1 - \cos\phi_2)]}{\cos(\phi_2 + \theta)}$$

Hotta et al (1974)

Capillary force $\qquad F_c = \pi \gamma \rho_2 \dfrac{\rho_1 + \rho_2}{\rho_1}$

Adams & Perchard (1985)

Viscous force $\qquad F_v = \dfrac{6\pi \eta \left(R^*\right)^2 V_n}{S}$

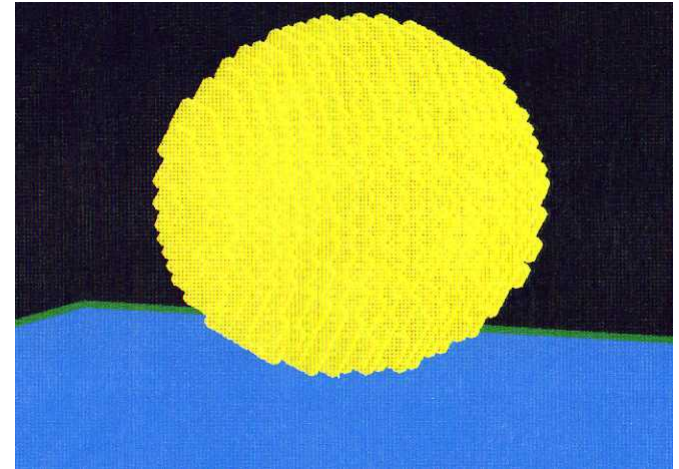Body-centred cubic array of 4062 primary spheres, d = 60 μm
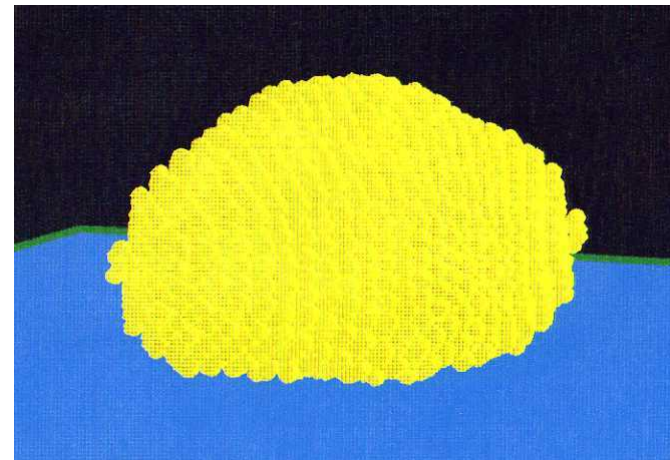
ρ = 2.65 Mg/m³   E = 70 GPa   ν = 0.3 μ = 0.3

pendular liquid bridges

surface tension = 25 mn/m

bridge volume = 1.13x10⁻¹⁰ ml (S = 0.71%)

impact velocity = 2 m/s

viscosity = 0

viscosity = 0.1 Pa.s
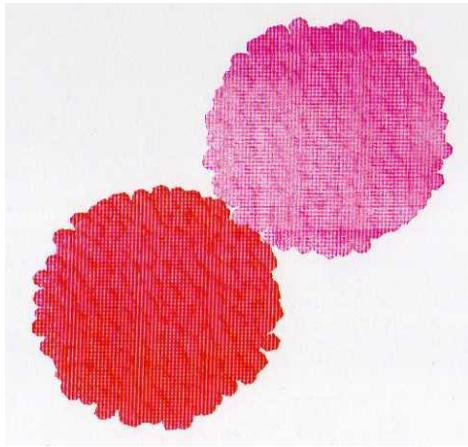
Thornton, Lian & Adams (1993)

WET AGGLOMERATE COLLISIONS

1000 particles in each agglomerate

D = 0.38mm   ‹d› = 60μm

η = 0.01 Pa.s   γ = 0.025 N/m

normal impacts θ = 0°

initial
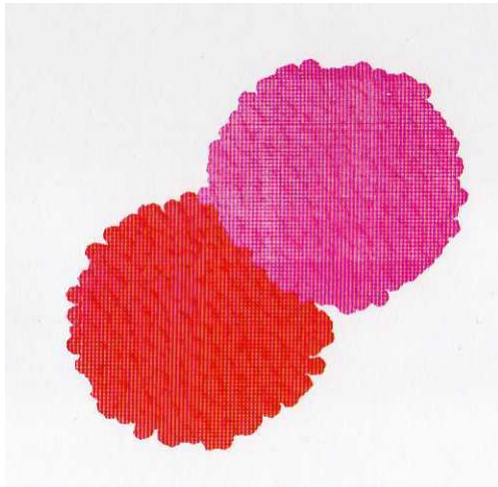
V = 1.0 m/s
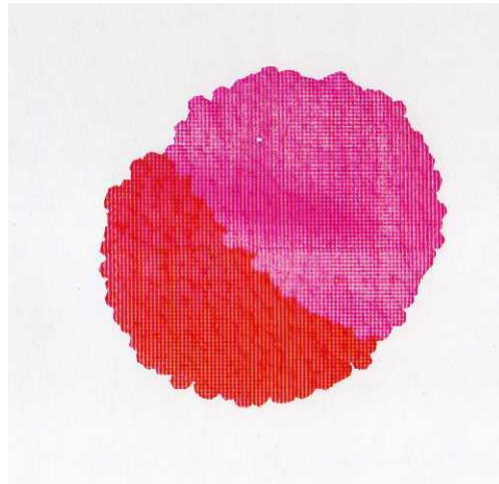
V = 2.0 m/s
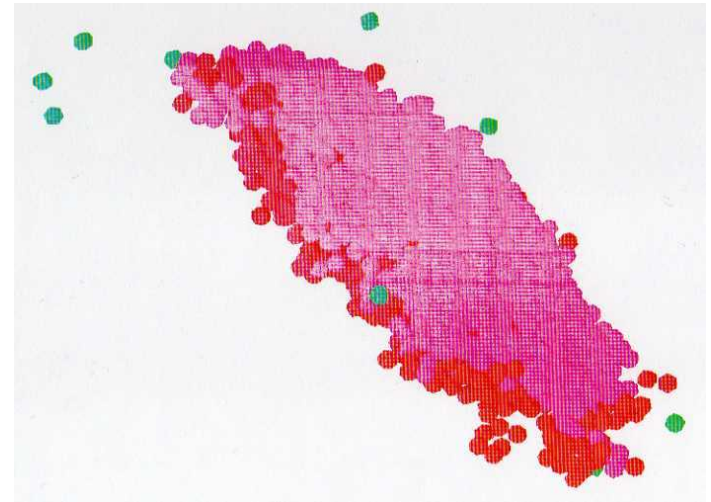
V = 5.0 m/s

OBLIQUE IMPACTS V = 5.0 m/s

θ = 0°

θ = 15°

θ = 30°

θ = 45°

θ = 60°

θ = 75°
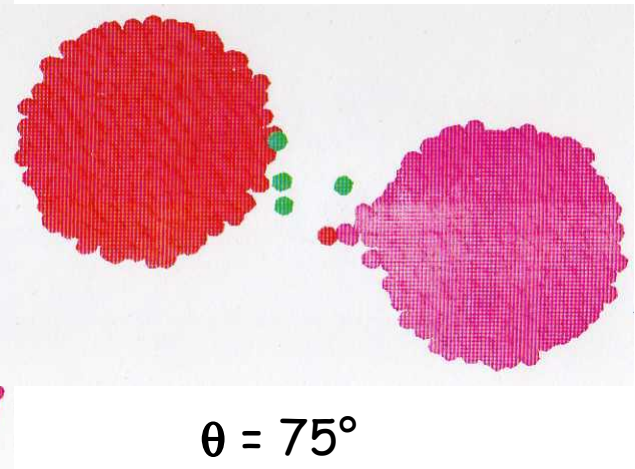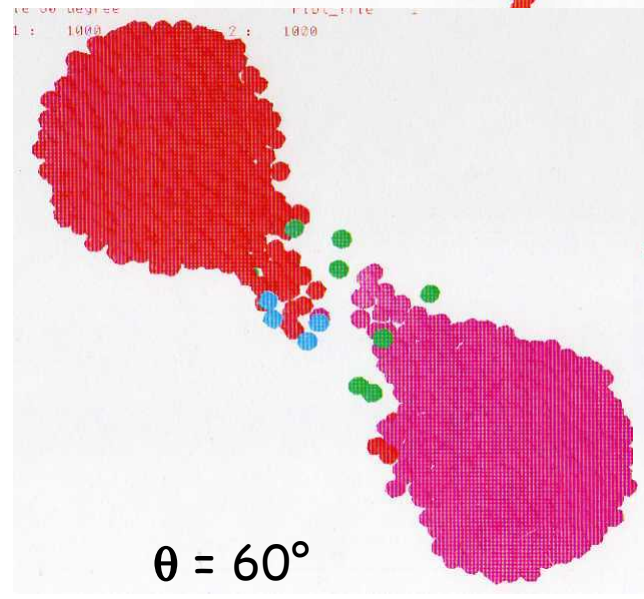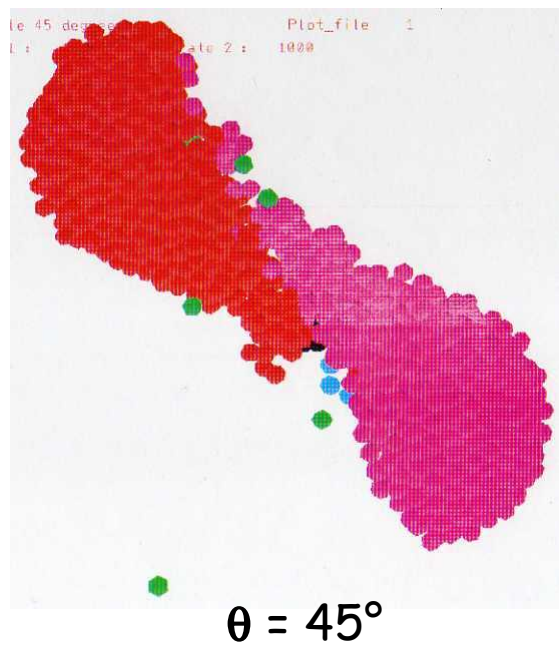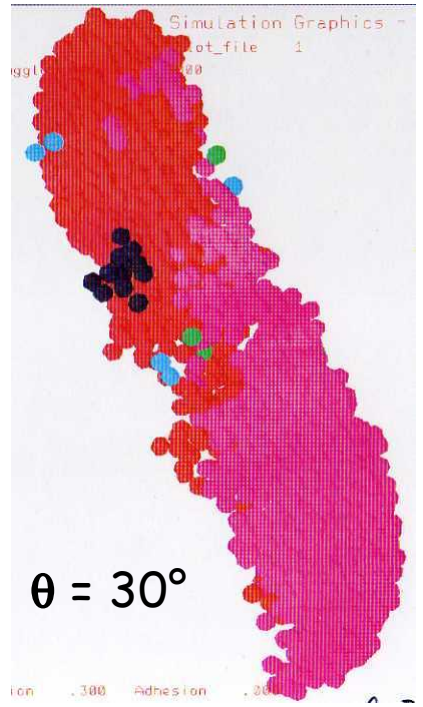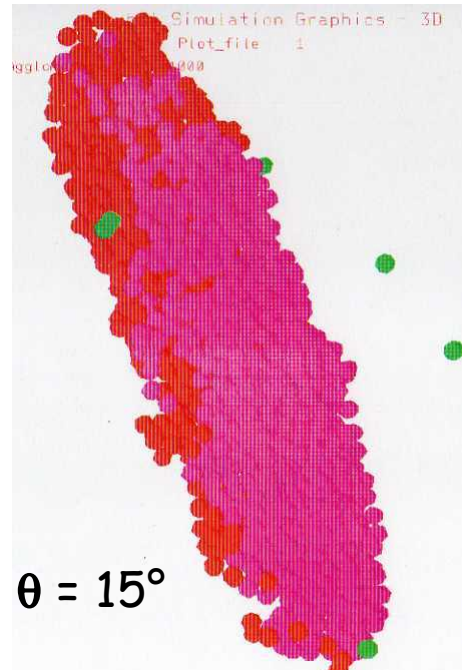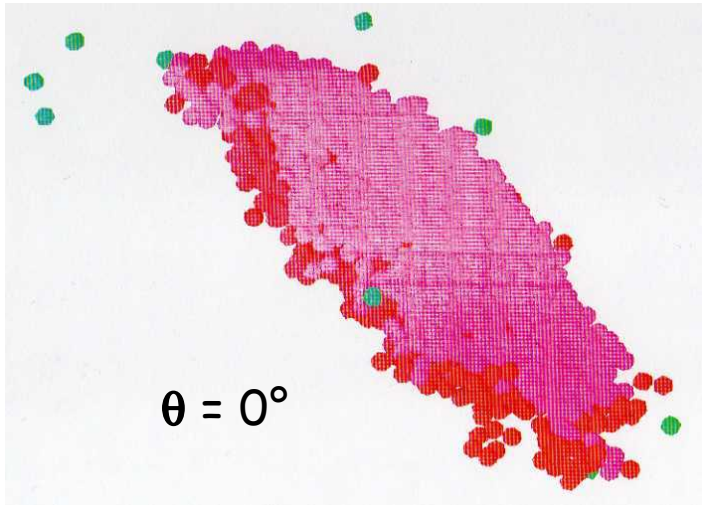
PARTICLE-FLUID INTERACTIONS

Kafui, Thornton & Adams (2002)

particle equations of motion

total force acting on particle i $f_i = f_{ci} + f_{fpi} + m_i g = m_i \ddot{x}_i$

torque applied to particle i $T_i = I_i \ddot{\theta}_i$

fluid-particle interaction force $f_{fpi} = -V_{pi} \nabla p + V_{pi} \nabla \cdot \tau_f + \boxed{\varepsilon f_{di}}$

fluid continuity and momentum equations

$$\frac{\partial(\varepsilon \rho_f)}{\partial t} + \nabla \cdot (\varepsilon \rho_f u) = 0$$

$$\frac{\partial(\varepsilon \rho_f u)}{\partial t} + \nabla \cdot (\varepsilon \rho_f u u) = -\nabla p_f + \nabla \cdot \tau_f - F_{fp} + \varepsilon \rho_f g$$

total fluid-particle interaction force per unit volume $F_{fp} = \dfrac{\sum_{i=1}^{n_c} f_{fpi}}{\Delta V_c}$

volume of computational fluid cell

drag force $\quad f_{di} = \dfrac{1}{2} C_{Di} \rho_f \dfrac{\pi d_{pi}^2}{4} \varepsilon_j^2 |u_j - v_i|(u_j - v_i)\varepsilon_j^{-(\chi+1)}$

fluid drag coefficient for a single unhindered particle $\quad C_{Di} = \left[0.63 + \dfrac{4.8}{Re_{pi}^{0.5}}\right]^2$

$\varepsilon_j^{-(\chi+1)} \quad$ corrects for the presence of other particles

and the dependence on the flow $\quad \chi = 3.7 - 0.65\exp\left[-\dfrac{(1.5 - \log_{10} Re_{pi})^2}{2}\right]$

particle Reynolds number $\quad Re_{pi} = \dfrac{\rho_f d_{pi} \varepsilon_j |u - v|}{\mu_s}$

3D fluidised bed simulations
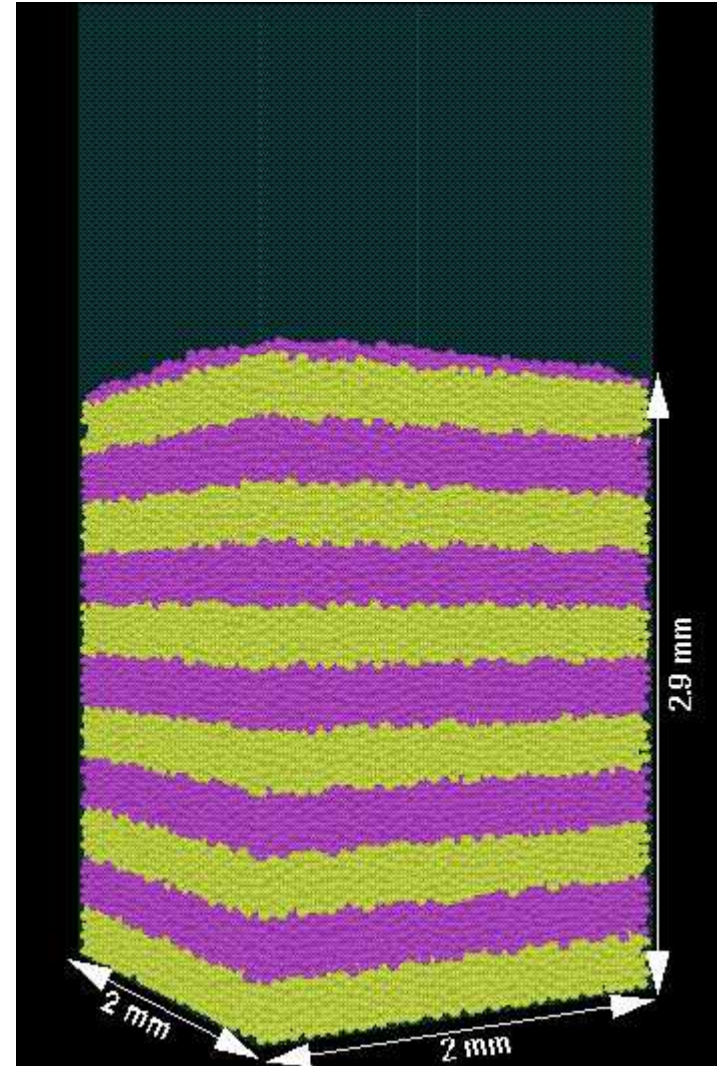
100,000 particles

fixed bed size 2 mm sq. x 2.9 mm high

(40d_p sq x 58 d_p)

bed void fraction   0.404

coordination number   4.71

total number of fluid cells 5000
(10x10x50)

fluid cell size   4 d_p cube

References

Adams MJ, Perchard V (1985). Chem. Eng. Symp. Series, 91, 147-160.

Derjaguin BV,Muller VM, Toporov YP (1975). J Colloid Interface Sci 53, 314-326

Fisher RA (1926). J. Agricultural Sci. 16, 492-505.

Goldsmith W, Lyman PT(1960). ASME J Appl Mech 27, 717-725.

Hotta K, Takeda K, Iinoya K (1974). Powder Technol. 10, 231-242.

Johnson KL (1976). Proc 4th IUTAM Congress, (Koiter, ed.) North-Holland, p 133

Johnson KL (1985). Contact Mechanics, Cambridge University Press

Johnson KL (1997). Proc Roy Soc London A 453, 163-179

Johnson KL, Kendall K, Roberts AD (1971). Proc Roy Soc London A 324, 301-313

Kafui KD, Thornton C (1996). Proc. 5th World Congress on Chem. Engng., San Diego.

Kafui KD, Thornton C, Adams MJ (2002). Chem. Eng. Sci. 57, 2395-2410.

Li L-Y, Wu C-Y, Thornton C (2002). IMechE C, J Mech Eng Sci 216,421-431

Lian G, Thornton C, Adams MJ (1992). J. Colloid Interface Sci. 88, 117-128.

Maugis D (1992). J Colloid Interface Sci 150, 243-269

Mesarovic SDJ, Johnson KL (2000). J Mech Phys Solids 48, 2009-2033.

Mindlin RD (1949). J. Appl. Mech. 16, 259-268.

Mindlin RD, Deresiewicz H (1953). ASME J Appl Mech 20, 327-344

Mishra BK, Thornton C (2002). Adv Powder Technol 13, 25-41

Samini A (2003) PhD thesis, University of Surrey

Samini A, Hassanpour A, Ghadiri M (2005). Chem Eng Sci 60, 3993-4004

Savkoor AR, Briggs GAD (1977). Proc. Roy. Soc. London A 356, 103-114.

Thornton C (1991). J. Phys. D: Appl. Phys. 24, 1942-1946.

Thornton C (1997). ASME J Appl Mech 64, 383-386

Thornton (1999) Mechanics of Granular Materials – an introduction (Oda & Iwashita, eds.) Balkema, 207-217.

Thornton C (2000). Constitutive Modelling of Granular Materials (Kolymbas, ed.), Springer, 193-208.

Thornton C, Ning Z (1998). Powder Technol. 99, 154-162

Thornton C, Randall CW (1988) Micromechanics of Granular Materials (Satake & Jenkins, eds.), Elsevier, 133-142

Thornton C, Yin KK (1991). Powder Technology 65, 153-166.

Thornton C, Lian G, Adams MJ (1993) Proc.2nd Int. Conf. on Discrete Element Methods, Cambridge, Massachusetts, 177-187.

Thornton C, Ning Z, Wu C-Y, Nasrullah M, Li L-Y (2001). Granular Gases (Pöschel & Luding, eds.) Springer, 184-194.

Wu C-Y (2001). PhD thesis, Aston University.

Wu C-Y, Li L-Y, Thornton C (2003). Int J Impact Engng 28, 929-946

Wu C-Y, Thornton C, Li L-Y (2007). Paper in preparation